Validation of 3D MHD simulations of mixed Ne-D_2 shattered pellet injection against H-mode experiments in JET

D. Bonfiglio[1,2], D. Hu[3], M. Kong[4], E. Nardon[5], F.J. Artola[6], A. Boboc[4], P. Carvalho[4], M. Hoelzl[7], S.-J. Lee[8], U. Sheikh[9], S. Silburn[4], B. Stein-Lubrano[10], R. Sweeney[10], G. Szepesi[4], the JOREK team and JET contributors

[1] *Consorzio RFX, Padova, Italy* [2] *CNR-ISTP Padova, Italy* [3] *Beihang University, Beijing, China* [4] *UKAEA-CCFE, Culham Science Centre, Abingdon, UK* [5] *CEA, IRFM, Saint-Paul-lez-Durance, France* [6] *ITER Organization, Saint-Paul-lez-Durance, France* [7] *Max Planck Institute for Plasma Physics, Garching b. M., Germany* [8] *Seoul National University, Seoul, Korea* [9] *École Polytechnique Fédérale de Lausanne (EPFL), Swiss Plasma Center (SPC), Lausanne, Switzerland* [10] *Massachusetts Institute of Technology, Cambridge, USA*

Introduction. Shattered pellet injection (SPI) is the technique selected for disruption mitigation in ITER, and is being tested in several tokamaks including JET [1]. In this work, we present results of nonlinear 3D MHD simulations of mixed Neon-Deuterium (Ne-D_2) SPI into H-mode JET plasmas, and their validation against experiments. We consider a medium size pellet with 8.1 mm diameter and we focus on the pre-thermal quench and thermal quench (TQ) phases. Simulations are performed with the 3D MHD code JOREK [2] using parameters as close as possible to experimental conditions. A scan in the pellet mixture ratio is carried out as done in JET [3]. Here, we focus on a pure Ne simulation and the comparison with three nominally identical reference JET-ILW pulses terminated by pure Ne SPI (#95709, #95711 and #95702).

Numerical setup. Free boundary JOREK simulations are performed with realistic (although axisymmetric) JET vessel and including poloidal field coils and diagnostic saddle coils. MHD equations are solved assuming separate electron and ion temperatures and a realistic plasma resistivity up to $T_e = 0.7$ keV (and uniform above this threshold). Distributions for the sizes and velocities of fragments in the SPI plume are consistent with laboratory measurements [4]. An average fragments velocity of 200 m/s is assumed, equal to the typical velocity of 8.1 mm pellets fired with mechanical punch [5]. An artificially large toroidal extent of $\Delta\phi = 0.5$ rad is assumed for the ablated gas cloud from each fragment, due to the limited resolution in toroidal Fourier harmonics (up to $n = 10$). Radiation from ablated Ne impurities is computed assuming a coronal equilibrium distribution of charge states (the non-equilibrium treatment of Ref. [6] will be addressed in the future). The JOREK mesh on the poloidal plane and the simulated SPI plume at 3 ms after exit from the shatter tube are shown in Fig. 1.

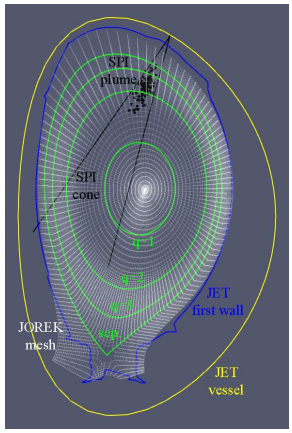

Figure 1: *JOREK mesh.*

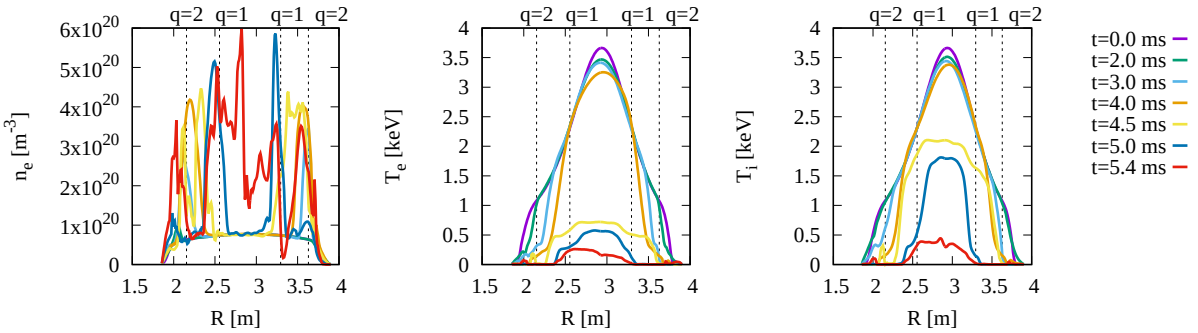

Figure 2: *Pure Ne simulation: temporal evolution of density and temperature midplane profiles.*

Pure Ne simulation: midplane profiles. The temporal evolution of density and temperature profiles along the midplane are shown, for the pure Ne SPI simulation, in Fig. 2. The initial simulation time $t = 0$ corresponds to the time when the fragments exit from the shatter tube. The electron density is found to increase significantly on the magnetic surfaces crossed by the ablating Ne fragments. At the same time, radiation from the ablated impurities cools down the plasma so that a cold front travels from the edge towards the core. This progressively induces MHD modes (and the related magnetic field stochastization) by both the helical cooling and current contraction mechanisms, as discussed in Ref. [7]. Then, after $t = 4$ ms, global magnetic field stochastization occurs and triggers a rapid (although not complete) first loss of the core temperature associated to the thermal quench. Electrons are more sensitive than ions to this stochastic transport channel, and indeed the core T_e drops more significanly than T_i. A final thermal collapse follows after $t = 5$ ms, when electron density starts to accumulate in the core.

Pure Ne simulation: validation against JET. The temporal evolution of main quantities for the pure Ne simulation, and the corresponding JET signals, are shown in Fig. 3. Time offsets are applied to JET signals so that the fragments exit the shatter tube at $t = 0$ as in JOREK.

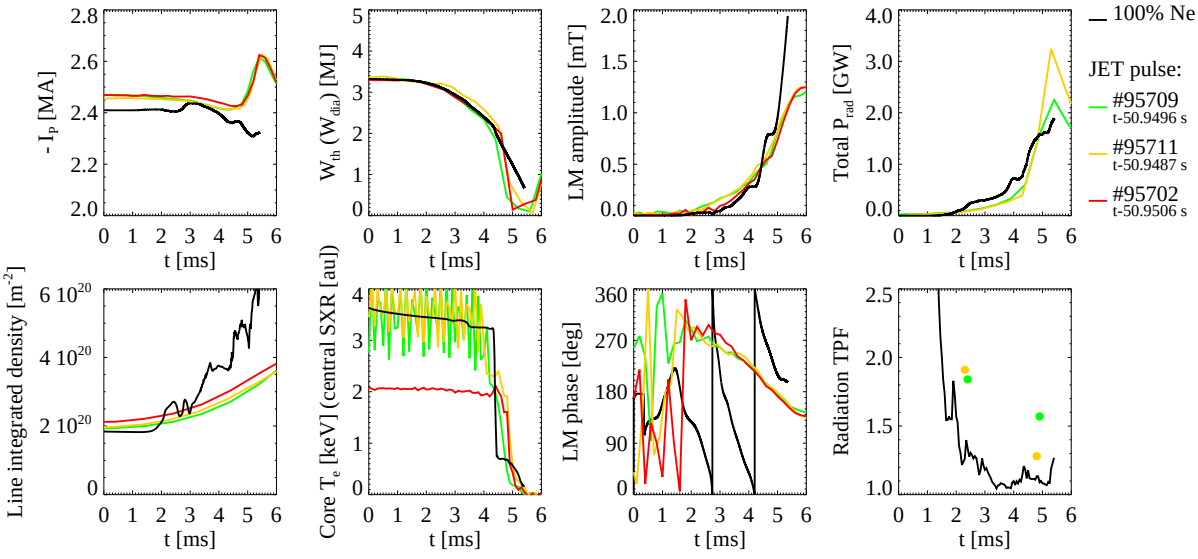

Figure 3: *Pure Ne simulation: temporal evolution of main quantities and comparison with JET.*

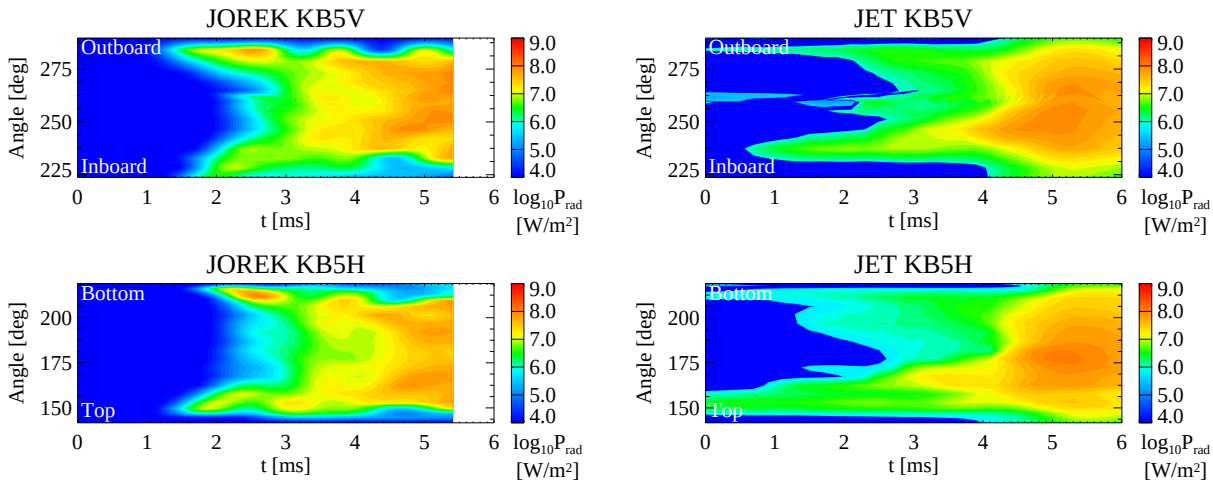

Figure 4: *Pure Ne simulation: synthetic bolometry and comparison with JET pulse #95709.*

The experimental line integrated density (from a central vertical chord away from the injection location) is measured by the polarimeter. The experimental total radiated power and radiation toroidal peaking factor (TPF) are derived from radiation structures that best fit KB5V and KB5H bolometry data at corresponding times, chosen from a pool of candidate structures using the Emis3D tool [3], according to physical assumptions for radiation structures away from the toroidal locations of bolometer arrays. Overall agreement is found between the JOREK simulation and reference JET pulses, especially concerning quantities related to the plasma thermal content and radiation. The time of the core T_e drop in the simulation matches very well the experimental TQ times (identified by the drop in the central chord SXR signal). Nonetheless, some discrepancies are observed. In particular, in the JOREK simulation the I_P spike is missing, the line integrated density at the TQ is overestimated, and the locked mode rotates significantly faster than what observed in JET (yet in the same direction and with a similar amplitude).

Pure Ne simulation: synthetic bolometry. Synthetic bolometry measurements with same low-pass filter, toroidal positions and lines of sight of vertical and horizontal JET bolometers (KB5V and KB5H) are shown in Fig. 4 together with the corresponding experimental measurements for pulse #95709. A similar comparison between synthetic and experimental bolometry measurements is performed for a massive gas injection-triggered JET disruption in Ref. [8]. Qualitative agreement is observed between the synthetic and experimental radiation patterns, in particular in the pre-TQ phase (between 2 and 3 ms) where both bolometers see radiation mainly coming from the plasma periphery. In this phase, the dominant radiation in JOREK comes from the outboard KB5V channels and bottom KB5H channels, whereas the opposite occurs in the experiment. This points out to possible differences in the parallel expansion of impurities.

Pure Ne simulation: 3D radiation structures. The radiation patterns from synthetic bolometry can be interpreted by looking at the evolution of the 3D radiation structures in JOREK, as

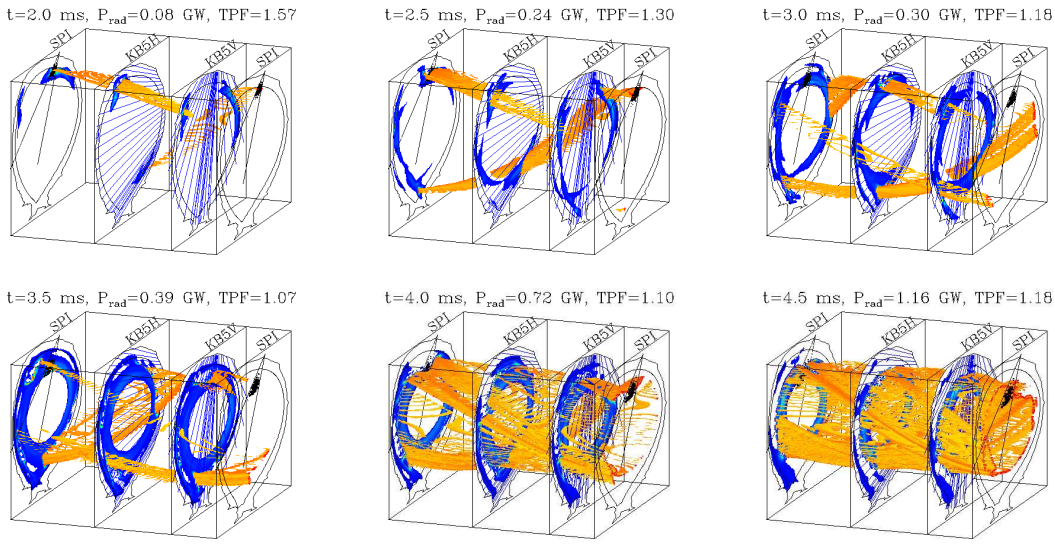

Figure 5: *Pure Ne simulation: temporal evolution of 3D radiation structures along the rectified torus.*

shown along the rectified torus in Fig. 5, where the isosurfaces corresponding to the peak power density of 10^8 W/m^3 are depicted in orange. In the early pre-TQ phase ($t = 2.5$ ms) the radiation comes from "fresh" impurities expanding along the flux tube connected with the ablating SPI fragments, and is consistent JET fast camera images. Between 3 and 4 ms, the radiating flux tube rotates poloidally due to the corresponding rotation towards the outboard midplane of the previously ablated material. A similar movement towards the outboard midplane was observed for off-midplane injection both numerically [9] and experimentally (in DIII-D) [10], but is not apparent from JET fast camera images for reference pulses. During the TQ phase (after $t = 4$ ms) the radiation is mainly associated with a cold 2/1 magnetic island with increasing width.

Extensions of this work will address further improvements of the numerical model and the validation against future SPI experiments in JET with upgraded SPI and diagnostic systems.

This work has been carried out within the framework of the EUROfusion Consortium, funded by the European Union via the Euratom Research and Training Programme (Grant Agreement No 101052200 - EUROfusion). Views and opinions expressed are however those of the author(s) only and do not necessarily reflect those of the European Union or the European Commission. Neither the European Union nor the European Commission can be held responsible for them. This work was carried out using the EUROfusion High Performance Computer Marconi.

References

[1] S. Jachmich *et al* 2022 Nucl. Fusion **62** 026012 [2] M. Hoelzl *et al* 2021 Nucl. Fusion **61** 065001

[3] U. Sheikh *et al* 2021 Nucl. Fusion **61** 126043 [4] T. E. Gebhart *et al* 2021 Fusion Sci. Technol. **77** 33

[5] L. R. Baylor *et al* 2021 Nucl. Fusion **61** 106001 [6] D. Hu *et al* 2021 Plasma Phys. Control. Fusion **63** 125003

[7] D. Hu *et al* 2018 Nucl. Fusion **58** 126025 [8] E. Nardon *et al* 2021 Plasma Phys. Control. Fusion **63** 115006

[9] H. R. Strauss and W. Park 1998 Phys. Plasmas **5** 2677 [10] R. Sweeney *et al* 2021 Nucl. Fusion **61** 066040